Int J Cardiovasc Imaging (2011) 27:259–269
DOI 10.1007/s10554-010-9793-y

ORIGINAL PAPER

Assessment of coronary stent by optical coherence tomography, methodology and definitions

Emile Aziz Mehanna · Guilherme Ferragut Attizzani · Hiroyuki Kyono · Michael Hake · Hiram Grando Bezerra

Received: 10 December 2010 / Accepted: 30 December 2010 / Published online: 19 February 2011

Abstract Optical coherence tomography has emerged as a powerful tool for stent assessment, and in a short time, has become the modality of choice for studying stent and vascular interactions in vivo. In this review, we discuss qualitative and quantitative parameters used for stent assessment by OCT. Various qualitative/quantitative variables of stent assessment are discussed in the perspective of the clinical and research values of each of them.

Keywords Optical coherence tomography · OCT · Coronary stent · PCI

Introduction

Optical Coherence Tomography's (OCT) high spatial resolution, combined with the blood-free environment, are substantial advantages for the study of coronary stents, when compared to previous technology, like intravascular ultrasound (IVUS). A sharp delineation of the lumen contour allows for easy image interpretation and fully-automated lumen area segmentation, with virtually no observer interference [1]. Moreover, detailed stent-strut evaluations can be performed for the first time, in vivo, with high inter- and intra-observer reliabilities [2]. Important features of baseline stent implantation can be well depicted by OCT, such as the measurement of stent area and diameters, as well as the detection of dissections and stent strut malapposition, as opposed to IVUS [3]. Furthermore, this tool enables detailed evaluation of tissue coverage in follow-up analysis [4]. This specific parameter has been used as a surrogate endpoint in several recently published drug-eluting stent (DES) trials [5–7]. Therefore, intravascular OCT may become the modality of choice for stent analysis in both the clinical and research areas.

The aim of this review is to describe in detail the aspects of stent assessment by OCT, highlighting particular features of both online analysis in the catheterization laboratory setting and offline detailed analysis for research purposes.

Proper imaging: a prerequisite for analysis

The methodology of OCT image acquisition has been described [8, 9]. One of the main challenges during this process, especially for first-time OCT users, is to accomplish proper imaging of the full stent length. We propose an easy method to assure total stent

Hiram G Bezerra received honoraria grant from St. Jude Medical.

E. A. Mehanna · G. F. Attizzani · H. Kyono · M. Hake · H. G. Bezerra (✉)
Harrington-McLaughlin Heart and Vascular Institute, University Hospitals Case Medical Center, Case Western Reserve University School of Medicine, Cleveland, OH, USA
e-mail: hiram.bezerra@UHhospitals.org

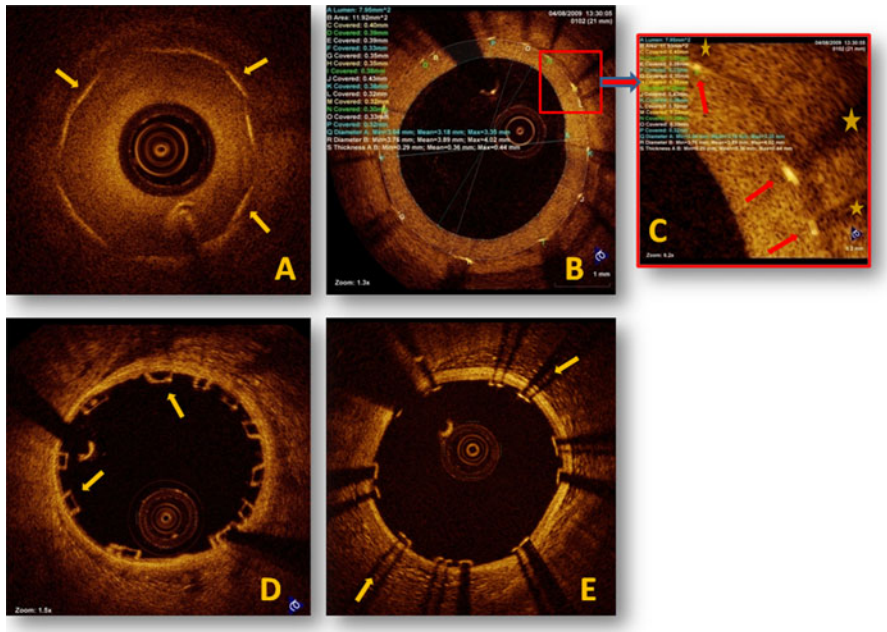

Fig. 1 Coronary stents by OCT. **a** Stent struts (*arrows*) are visible before luminal blood clearance. **b** Stent follow up case with typical strut distribution pattern. **c** Commercially available (BMS and DES) stent strut appearance consists of blooming (*arrow*) and shadow (*star*). **d** BVS stent with "boxed appearance" of individual stent struts (*arrows*). **e** Typical "tram trail" pattern of shadow (*arrows*) behind struts of NEVO stent

assessment: it is well known that adequate assessment of stents by OCT requires a blood-free environment; however, the high signal reflection generated by the metallic stent strut can be identified through blood (Fig. 1a). This property can be used clinically to allow proper positioning of the imaging catheter distal to the area of interest in a way to cover the full stent length while imaging. The catheter can be advanced until the disappearance of stent struts, which indicates that the distal edge of the stent has been crossed. The automated pullback, with proper coronary flushing, can then be initiated.

The pullback length of the current FD-OCT is fixed to 54 mm, while the speed of the pullback may be adjusted between 10 and 20 mm/s. Multiple pullbacks might be needed to cover long lesions with multiple stents; hence, until a new generation of catheters become available with longer pullback lengths, fiduciary markers, such as side-branches, should be used for co-registration, if multiple pullbacks are required.

Image analysis

Image analysis can be directly performed on the imaging console in the catheterization laboratory immediately after the pullback is taken, seeking both qualitative assessment (such as identification of dissections, tissue prolapse, stent expansion and malapposition) and quantitative measurement of stent area. Due to the sharp interface between the lumen and vessel wall, full volumetric segmentation of the lumen can also be obtained online.

When used for research purposes, detailed offline strut-level analysis can be performed and will be carefully described later on in this article. For stent follow-up, the high resolution of OCT gives this modality a clear edge on IVUS, especially in quantitative assessment of neointimal hyperplasia (NIH). The tendency of IVUS to underestimate NIH has been well-documented [4, 10].

Image preparation

Z-offset calibration

Before any measurements can be made, the image should be calibrated via adjustment of the Z-offset. This corrects for the difference in the optical path length between the sample and reference arm [1]. In the FD-OCT catheters, a semi-transparent catheter around the optic fiber is more suitable for direct calibration.

When calibrating the image, it is expected that the calibration affects the entire image uniformly,

provided that the wire is centrally located in the lumen. It is important, however, to make sure that the Z-offset is corrected on individual cross-sections selected by operators to guide PCI in the catheterization laboratory.

In fact, we found that a 1% change in the magnitude of the ideal Z-offset from the optimal Z-offset can result in a 6–7% error in diameter and a 12–14% error in area measurements. Small changes in magnitude can also amplify the contour distortion, which may result in misinterpretation of the image. This is mostly true in cases in which the wire is located in an eccentric position [11].

Index of refraction

Adequate blood clearance is essential for good stent assessment. This is usually achieved by means of injection of undiluted contrast (100%). However, if other media or diluted contrast are used, the refraction index of each of these solutions must be known and set in the machine before any measurement is performed, since they will impact the final values.

Stent appearance by OCT

Stent struts have a unique signature in OCT. The majority of commercially available stents (whether bare metal stents (BMS) or drug eluting stents (DES)) have a metallic frame. Light fully reflects (specular reflection) on the surface of stent struts creating a hypersignal, usually named as "blooming". Due to the inability of light to pass through metal, a shadow can be seen behind the blooming. Although this phenomenon is also true for IVUS, it is more obvious with OCT because of the higher resolution of the method. The operator must be aware of this phenomenon in order to avoid overcalling malapposition. Both features (blooming and shadow) help in the identification of individual struts, a step needed for qualitative and quantitative analysis of OCT images (Fig. 1b, c).

As opposed to metallic stents, light can penetrate polymer and bioresorbable vascular scaffold stents (BVS) (Abbott Vascular, Santa Clara, California), which can be imaged volumetrically by OCT. BVS struts appear as "boxes" with clear delineation of strut borders at implantation (Fig. 1d). This allows a proper assessment of BVS deployment, as well as stent degradation and neointima formation at follow-up since the "box appearance" persists until total degradation of the polymer [12].

Other unique stent designs, like NEVO^{TM}, (Cordis Corporation, Johnson & Johnson, Warren, NJ) a sirolimus-eluting stent with a biodegradable polymer and reservoir technology have a unique "tram trail" appearance by OCT created by the ability of light to pass through the polymer reservoir (Fig. 1e).

Clinical assessment of stents

In the following section, we will briefly discuss the main parameters which are collected online intra-procedure and can be readily available in the catheterization lab suite.

Stent expansion and malapposition

The evaluation of stent underexpansion is of particular importance in the clinical setting since it has been previously related to stent failure [13, 14]. Furthermore, stent strut malapposition, defined as the lack of contact between stent struts and the underlying vessel wall in a non-bifurcated segment, can also be well depicted by OCT imaging in the catheterization laboratory immediately after stent implantation (Fig. 2a). OCT is more sensitive and accurate for stent malapposition detection as compared to IVUS [3].

The concept of OCT evaluation is similar to that of IVUS on a cross sectional level. However, the blood free environment obtained with OCT creates a sharp interface between the lumen and vessel wall and facilitates the autosegmentation of the lumen and results in easier image interpretation [15]. The stent contour can then be traced using the detected stent struts as anchor points and interpolating the tracing in areas with absences of stent struts—fully-automated stent segmentation algorithms are currently being developed.

Comparisons between OCT and IVUS have been made and "validated" by histomorphometry [4]. Acknowledging the fact that pathology is an imperfect gold standard, since tissue processing may impose significant changes in the vessel, we have evaluated FD-OCT and IVUS by means of a phantom model [16]. Although there was correlation between the modalities, OCT proved to be more precise with minimal variability.

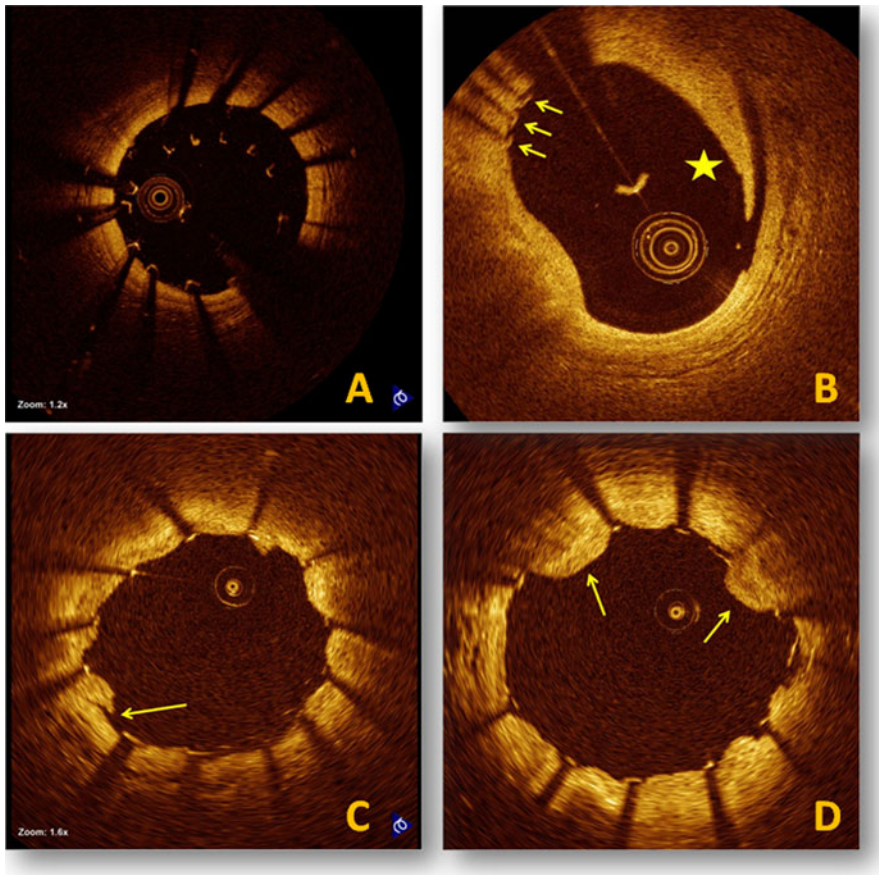

Fig. 2 Findings at stent implantation. **a** Underexpanded stent with malapposed struts. **b** Edge dissection: dissection flap (*star*) and stent struts (*arrows*) are observed. **c** Dissection in stented segment: *arrow* corresponds to disruption of luminal vessel surface between stent struts. **d** Tissue prolapse between stent struts (*arrows*)

The evaluation of neointima thickness (NIT) in follow-ups of stent implantations can be performed with great accuracy by OCT when compared to histology [17]. In situations of large amounts of NIH; i.e. bare metal stents and less potent drug eluting stent like Endeavor™ (Medtronic CardioVascular, Santa Rosa, California), OCT measurements correlate well with IVUS. However, OCT is clearly superior in depicting small amounts of NIH, in cases of potent drug eluting stents [5, 10]. We also demonstrated in a substudy of the ODESSA trial that 250 stented segments with no detectable NIH by IVUS had neointimal coverage ranging from 67–100% by OCT [18], thus reinforcing the need for a high resolution method for the appropriate study of the actual potency of drug-eluting stents.

Dissections

Edge dissection is defined as a disruption of the luminal vessel surface in the edge segment (within 5 mm proximal and distal to the stented region) (Fig. 2b). Dissection in the stented segment is a disruption of the luminal vessel surface, with a visible dissection flap in the segment covered by the stent struts (Fig. 2c).

The endothelial integrity is important in preventing thrombus deposition, and data from pathology has linked the disruption of the vessel continuity to stent thrombosis [19]. The diagnosis of edge and intra-stent dissections has been reported as 26.3 and 87.5%, respectively, in 73 consecutive patients evaluated by OCT imaging immediately after stent

implantation. However, no in-hospital event has been identified in this population [20]. These values are significantly higher as compared to edge dissections detected by IVUS (10.7%) [14]. The clinical significance of edge dissections identified by OCT still needs to be addressed by prospective trials, however, apparently, most of these are benign situations.

Tissue prolapse

The protrusion of tissue between adjacent stent struts towards the lumen, without disruption of the continuity of the luminal vessel surface is called tissue prolapse (Fig. 2d). Data obtained from IVUS studies have highlighted rates ranging from 16.6 up to 35% of tissue prolapse after stent implantation [21, 22]. Naturally, OCT's better assessment of the stent segment is able to detect some amount of tissue prolapse in almost all stented segments (98%) [20]. This result has been found to be similar to a postmortem evaluation [23]. As for edge dissections, the clinical impact of this finding, immediately after stenting, still needs to be better explored.

Abnormal intra stent tissue

Previous studies have shown the ability of OCT to detect intracoronary thrombi. They are characterized as masses protruding into the vessel lumen, and can be classified as red or white. Red thrombi consist primarily of red blood cells and are characterized by high signal attenuation, whereas white thrombi are composed largely of white blood cells and platelets, and are characterized by low signal attenuation. Kume et al. [24] used 1/2 width of signal intensity, defined as the distance from peak intensity to its 1/2 intensity, to explore the attenuation properties of the different thrombi (Figs. 3a, b). Other contributions in the setting of acute coronary syndrome, clearly demonstrated the potential of the method in identifying thrombi [25]. Nevertheless, the discrimination of thrombi from other potential abnormally-appearing intraluminal tissues remains ambiguous, particularly in stented vessels and stable patients. Residual blood, the result of inadequate blood clearance, fibrin and intimal flaps are examples of situations that can mimic thrombi. Thus, we endorse a conservative

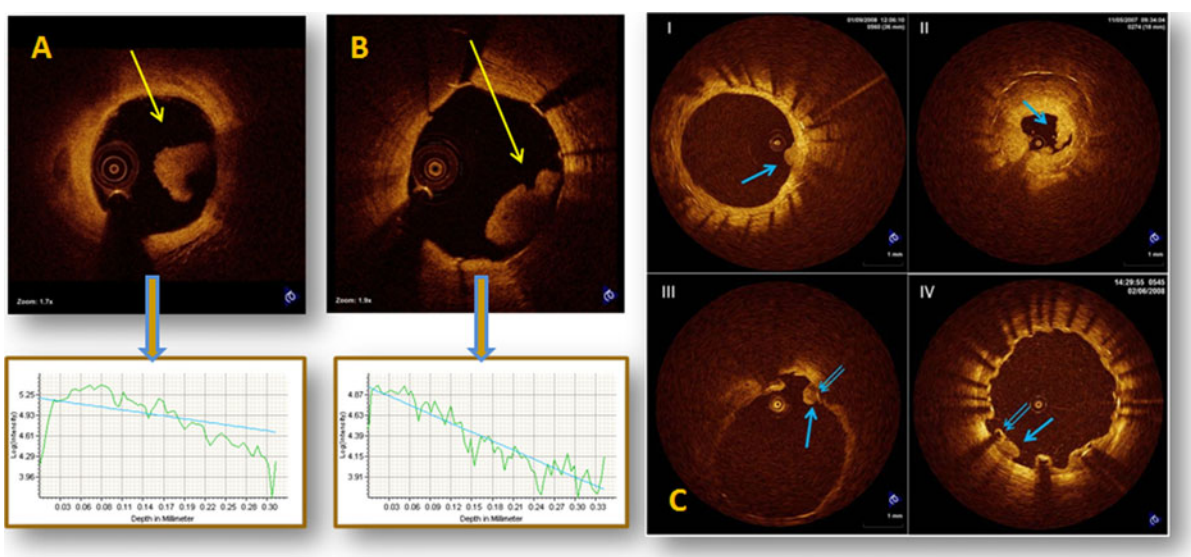

Fig. 3 Thrombus and AIT by OCT. **a** *White* and (**b**) *red* thrombus as seen by OCT. Note the sharper decrease in light intensity in the red thrombus compared to the white thrombus as depicted in corresponding graphs. **c** Representative images of abnormal intraluminal tissue (AIT). AIT was classified into 4 categories by their appearance, according to its relationship with strut coverage, apposition, presence of neointimal hyperplasia and location in a severely stenotic segment. I: AIT related with neointimal hyperplasia (Arrow-AIT type I). II: AIT related with tight stenosis (Arrow-AIT type II). Note that lumen area of this image is 0.92 mm^2. III: AIT related with uncovered stent (*Arrow*-AIT type III, Double arrow-Uncovered stent strut). IV: AIT related with malapposed struts (Arrow-AIT type IV, *Double arrow*-Malapposed stent strut)

approach when evaluating intraluminal structures that resemble thrombi and adopt the more descriptive term "abnormal intraluminal tissue" (AIT) to describe these structures, until more objective evidence emerges to guide accurate identification, as opposed to subjective interpretations.

We characterized AIT as intraluminal material attached to the vessel wall and protruding into the lumen with an irregular surface and significant light attenuation. AIT was further classified into 4 categories according to its relationship with strut coverage, apposition, presence of underlying NIH and location in a severely stenotic segment, to evaluate its relationship with other pathological conditions; I: neointima related, II: restenosis related (lumen area <1 mm^2), III: uncovered strut related and IV: malapposed strut related (Fig. 3c).

Strut level analysis of stents

The concept of high-risk of adverse outcomes associated with uncovered stent struts at follow-up has emerged from pathology studies which identified this feature as an independent predictor for stent thrombosis [26]. Moreover, larger areas of incomplete stent apposition were also correlated to the development of very late stent thrombosis [27]. Hence, the evaluation of the above-mentioned parameters after stent implantation is of particular importance. Unlike IVUS, which only evaluates at a cross-sectional level, OCT allows, for the first time, detailed in vivo assessment of each stent strut element, as a consequence of its higher resolution ($\sim$10 μm of axial resolution). Strut coverage is a novel and central parameter that has emerged as a primary endpoint for diverse recent clinical trials.

Strut classification

Our approach is to classify stent struts into 4 main categories: covered, covered-protruding (disturbing lumen contour, but covered), uncovered-apposed, and uncovered-malapposed. Strut coverage is qualitatively assessed, for the presence of any tissue that resembles NIH. If a strut is classified as uncovered (either no tissue or AIT), the distance between the superficial reflection and the lumen contour is subsequently measured to assess for malapposition. A strut will be classified as malapposed if the measured distance is superior to the nominal thickness of the stent strut. It is important to note that the real position of the inner surface of the stent strut falls in the center of the blooming (Fig. 4) [28]. Two methodologies have been used for quantitative strut level assessment: the first method consists of measuring the distance from the center of the blooming to the vessel wall [29, 30]. Another method consists of measuring the distance from the inner surface of the blooming to the vessel wall and correcting for half of the thickness of the blooming (18 μm) [11]. We prefer adopting the latter methodology since we previously

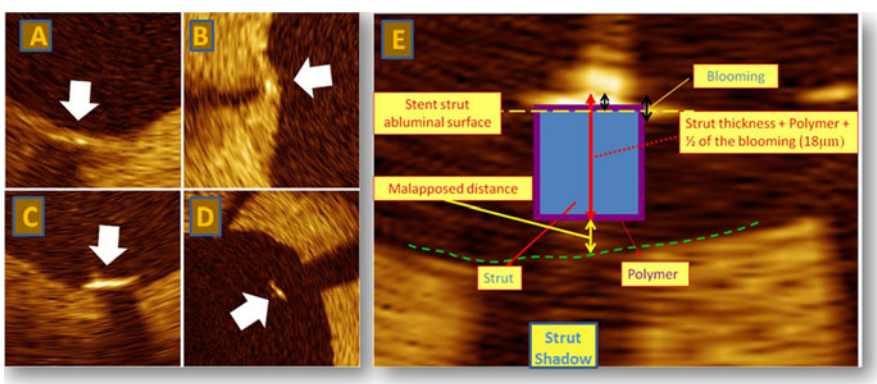

Fig. 4 Strut coverage classification and malapposition measurement. **a** Covered-embedded strut. **b** Covered-protruding strut. **c** Uncovered-apposed strut. **d**Uncovered-malapposed strut. **e** Malapposition is defined when the measured distance from the surface of the blooming to the lumen contour is higher than the total thickness of the stent strut + polymer + one-half of the blooming (the stent surface should be, theoretically, located at one-half the distance of the blooming thickness)

demonstrated high inter-observer agreement with this method (R = 0.997) [5].

Interval of analysis and variability

In practice to date, the majority of stent trials have utilized a frame analysis interval of 1 mm, while several trials have used an interval of 0.5 mm [31, 32]. We have reported that large intervals (0.5–1 mm) are suitable for area assessment (Table 1). On the other hand, a small analysis interval is highly recommended for strut coverage assessment, since a high variability may occur if large intervals are applied (Fig. 5) [33]. Qualitative assessment (dissection, protrusion, AIT, malapposition) should consider all the frames.

Table 1 Analyzed frame interval and area measurement

Minimal lumen area			Minimal stent area		
Interval	Variability	SD	Interval	Variability	SD
5*	0	0	5*	0	0
10	2.11	4.65	10	1.98	3.65
15	3.27	5.8	15	2.87	4.09
20	4.89	8.34	20	3.64	4.66
25	5.72	9.77	25	4.33	4.78
30	7.51	13.55	30	4.71	5.44
35	9.35	22.35	35	5.35	5.9
40	9.56	16.17	40	5.75	6.04

A low variability (<10%) was observed for minimal lumen and stent area measurements for all tested interval analyses. At the maximum tested interval (40 frames, 2.4 mm) the variability (%, SD) for minimal lumen and stent area was 9.6 ± 16.2, 5.8 ± 6, respectively

* Data obtained using TD-OCT

Whether assessment is done on a cross-sectional level or on a strut level, one of the main advantages of OCT over previous invasive imaging modalities is the high reproducibility of results obtained by different analysts or by the same analyst when analyzing the same image at different time points [2, 16, 34]. This is mainly due to the high resolution of the modality, which eases image interpretation and significantly reduces ambiguous calls during analysis, placing the method in a unique position for serial studies.

Special situations

Bifurcation

The evaluation of bifurcated segments demands special attention since the struts located in the ostium of the side branch are floating and never attached to the vessel wall. The longitudinal reconstruction of the

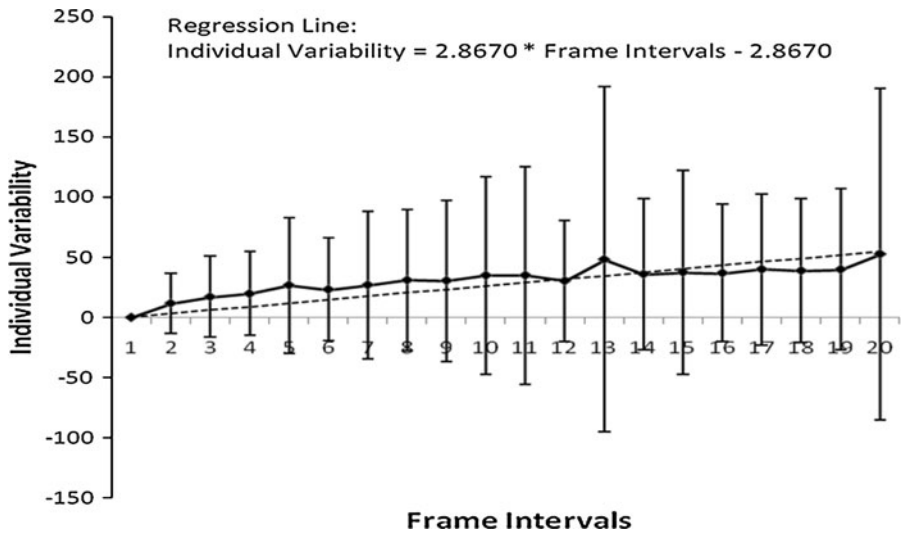

Fig. 5 Variability of strut coverage assessment according to the frame interval of analysis. For every frame interval increase (0.06 mm), a 2.9% increase in variability for quantification of % uncovered struts is expected. The variability reached an unacceptable 45% at 1 mm (15 frames) interval

vessel may help in defining the limits of the bifurcation.

We have proposed a methodology for bifurcation assessment that takes into consideration the opening angle of the side branch ostium in cross-sectional OCT images. In order to evaluate the axial tissue distribution after stent implantation, we have divided the segment of interest into three distinct regions. By means of this methodology, we have reported a variable pattern of strut coverage in the bifurcation among different stent technologies [35].

Overlap

Overlapping stents are readily identified by OCT as a two layer segment; however, a precise classification of the layers in a 2D image is not possible. ODESSA was the first trial using OCT to assess overlapping stents in human coronary arteries [5]. Since then, we performed a single stent cross-section contour by means of interpolation of the most external struts. Advanced 3D reconstruction of the overlap region may provide additional insights on the topic.

Pitfalls and artifacts seen in OCT imaging

While FD-OCT has eliminated many of the artifacts seen with TD-OCT, identification of these most common pitfalls in OCT imaging remains of critical importance for adequate image interpretation. In this section, we describe the major and minor pitfalls and artifacts that prevent ideal stent assessment by OCT.

Blood in catheter

Flushing the distal port of the catheter with contrast to displace blood from the catheter sheath is one of the key preparatory steps before image acquisition. Failure to do so results in an incomplete purge of the inner lumen of the imaging catheter. This may dim and blur a large section of the image (Fig. 6a). While stent and lumen areas can still be approximated in the clinical setting, such images should be excluded from formal offline analysis.

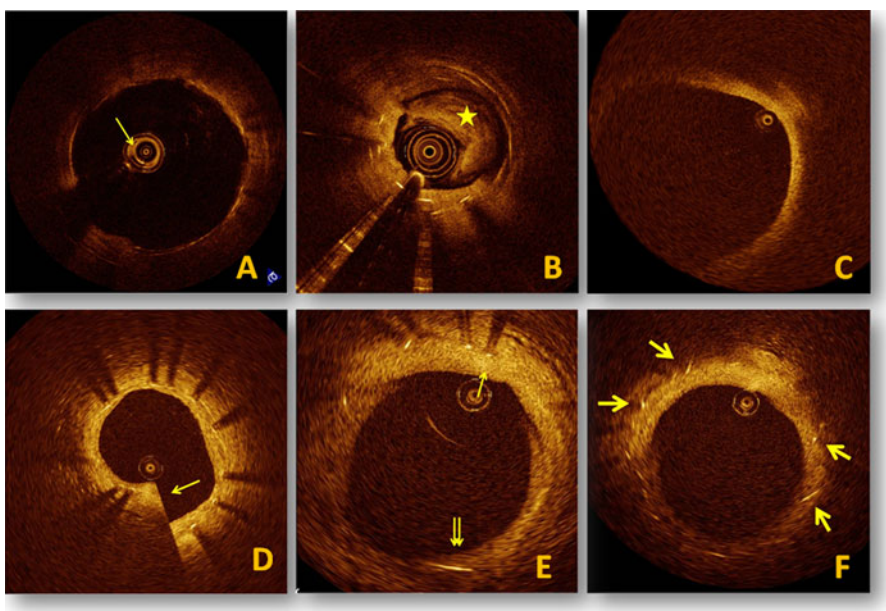

Fig. 6 Artifacts and Pitfalls. **a** Blood in imaging catheter (*arrow*) and in vessel lumen (*star*) **b** resulting in poor image quality. **c** Out of screen non analyzable cross sectional OCT image. **d** Sew-up artifact (*arrow*) due to rapid movement of artery or imaging catheter within a single frame. **e** Merry-Go-Round artifact. Stent strut located far from the imaging wire (*Double arrow*) appears longer in length than the strut located close to the imaging wire (*Arrow*) **f** Sun-flower artifact. Struts (*Arrows*) appear to align toward the image wire akin to the manner sunflowers align to the sun

Blood in lumen

Creating a blood free environment is one of the main challenges of OCT image acquisition. In first generation OCT systems (TD-OCT), blood clearance was achieved by proximal balloon occlusion and flushing of the vessel using the distal end holes of the occlusion balloon. Technological developments brought by FD-OCT, notably its high pullback speed, allowed a simpler method to clear blood. Contrast flushing (preferably via the power injector) creates the needed blood free environment for a few seconds, which is enough to acquire the image. Nevertheless, particularly in challenging anatomy (tortuosity, critical stenosis, diffuse disease…), residual blood in the lumen remains the major cause of poor image quality. Blood attenuates and may defocus the OCT light beam. This reduces the brightness of the vessel wall, especially at large radial distances from the light source (Fig. 6b). Images with residual blood should be excluded from formal offline analysis and care should be taken in the catheterization laboratory not to confuse any residual luminal blood artifacts with red thrombi, both of which have high attenuation indexes as previously described.

Out of screen

The scan diameter (field of view) is particularly limited in the first generation of TD-OCT. As a result, the scan range is ideal for vessels less than 3.75 mm in diameter. Because of this limit, large vessel images can extend out of the screen, which is one of the most common exclusion criteria of frame assessment in clinical trials (Fig. 6c). The current generation of OCT systems (FD-OCT) reduces the rate of out-of-screen images, since they have a larger field of view, $\sim$10 mm.

Sew up artifact

The artifact is caused by rapid movement of the artery or imaging catheter within a single frame, leading to single point misalignment of the lumen border (Fig. 6d). However, the frequency of this issue is decreased in current FD-OCT systems, since image acquisition is much faster than TD-OCT.

Artifacts related with the eccentric wire position

Eccentric wire position can lead to diverse artifacts and misinterpretations. Tissue classification is limited in this situation since we should expect an inverse relation between the distance from the source of the light and signal. In other words, the tissue closer to the catheter will look brighter as compared to the tissue on the opposite side even if they are essentially the same. The length of the strut element can be distorted due to the loss of lateral resolution in a position distant from the optimal focus (Fig. 6e). Distortion of the strut element reflection is also observed altering the strut orientation according to the angle of incidence of light (the "sunflower effect") (Fig. 6f) [11].

Future prospects: three-dimensional reconstruction

Three-dimensional (3D) visualization of OCT images has been described [36]. The faster the pullback, the less artifacts will be generated as a result of cardiac motion. However, for optimal 3D reconstruction, small frame intervals are necessary. We can expect that the development of even faster laser sources and very fast pullbacks at high frame rates will make 3D OCT reconstruction even more attractive and part of the routine interpretation.

In quiet a short time, OCT has become the standard imaging modality for stent analysis in the research environment. It is also not difficult to predict that the penetration of this modality in the clinical setting will rapidly increase. As a light-based technology, OCT will continue to quickly evolve, and hardware and software development will make the method even more attractive for stent assessment.

Conflict of interest None.

References

1. Bezerra HG et al (2009) Intracoronary optical coherence tomography: a comprehensive review clinical and research applications. JACC Cardiovasc Interv 2(11):1035–1046
2. Gonzalo N et al (2009) Reproducibility of quantitative optical coherence tomography for stent analysis. EuroIntervention 5(2):224–232

3. Rosenthal N et al. (2009) Comparison of intravascular ultrasound and optical coherence tomography for the evaluation of stent segment malapposition. J Am Coll Cardiol 53(A1–A99 (supplement))
4. Suzuki Y et al (2008) In vivo comparison between optical coherence tomography and intravascular ultrasound for detecting small degrees of in-stent neointima after stent implantation. JACC Cardiovasc Interv 1(2):168–173
5. Guagliumi G et al (2010) Optical coherence tomography assessment of in vivo vascular response after implantation of overlapping bare-metal and drug-eluting stents. JACC Cardiovasc Interv 3(5):531–539
6. Guagliumi G et al (2010) Strut coverage and vessel wall response to zotarolimus-eluting and bare-metal stents implanted in patients with ST-segment elevation myocardial infarction: the OCTAMI (Optical coherence tomography in acute myocardial infarction) study. JACC Cardiovasc Interv 3(6):680–687
7. Guagliumi G et al (2010) Strut coverage and vessel wall response to a new-generation paclitaxel-eluting stent with an ultrathin biodegradable abluminal polymer: optical coherence tomography drug-eluting stent investigation (OCTDESI). Circ Cardiovasc Interv 3(4):367–375
8. Guagliumi G, Sirbu V (2008) Optical coherence tomography: high resolution intravascular imaging to evaluate vascular healing after coronary stenting. Catheter Cardiovasc Interv 72(2):237–247
9. Takarada S et al (2010) Advantage of next-generation frequency-domain optical coherence tomography compared with conventional time-domain system in the assessment of coronary lesion. Catheter Cardiovasc Interv 75(2):202–206
10. Capodanno D et al (2009) Comparison of optical coherence tomography and intravascular ultrasound for the assessment of in-stent tissue coverage after stent implantation. EuroIntervention 5(5):538–543
11. Suzuki N et al. (2010) The impact of an eccentric intravascular image wire during coronary optical coherence tomography imaging. EuroIntervention (in press)
12. Onuma Y et al. (2010) Intracoronary optical coherence tomography and histology at 1 month and 2, 3, and 4 years after implantation of everolimus-eluting bioresorbable vascular scaffolds in a porcine coronary artery model. An attempt to decipher the human optical coherence tomography images in the ABSORB trial. Circulation
13. Kasaoka S et al (1998) Angiographic and intravascular ultrasound predictors of in-stent restenosis. J Am Coll Cardiol 32(6):1630–1635
14. Fujii K et al (2005) Stent underexpansion and residual reference segment stenosis are related to stent thrombosis after sirolimus-eluting stent implantation: an intravascular ultrasound study. J Am Coll Cardiol 45(7):995–998
15. Yamaguchi T et al (2008) Safety and feasibility of an intravascular optical coherence tomography image wire system in the clinical setting. Am J Cardiol 101(5):562–567
16. Tahara S et al (2011) In vitro validation of new Fourier-domain optical coherence tomography. EuroIntervention 6(7):875–882
17. Murata A et al (2010) Accuracy of optical coherence tomography in the evaluation of neointimal coverage after stent implantation. JACC Cardiovasc Imaging 3(1):76–84
18. Bezerra HG et al. (2009) Unraveling the lack of Neointimal hyperplasia detected by intravascular ultrasound using optical coherence tomography: lack of spatial resolution or a true biological effect? J Am Coll Cardiol 10 (Suppl A):90A
19. Farb A et al (2003) Pathological mechanisms of fatal late coronary stent thrombosis in humans. Circulation 108(14):1701–1706
20. Gonzalo N et al (2009) Optical coherence tomography assessment of the acute effects of stent implantation on the vessel wall: a systematic quantitative approach. Heart 95(23):1913–1919
21. Futamatsu H et al (2006) Characterization of plaque prolapse after drug-eluting stent implantation in diabetic patients: a three-dimensional volumetric intravascular ultrasound outcome study. J Am Coll Cardiol 48(6): 1139–1145
22. Kim SW et al (2006) Frequency and severity of plaque prolapse within Cypher and Taxus stents as determined by sequential intravascular ultrasound analysis. Am J Cardiol 98(9):1206–1211
23. Farb A et al (1999) Pathology of acute and chronic coronary stenting in humans. Circulation 99(1):44–52
24. Kume T et al (2006) Assessment of coronary arterial thrombus by optical coherence tomography. Am J Cardiol 97(12):1713–1717
25. Kubo T et al (2007) Assessment of culprit lesion morphology in acute myocardial infarction: ability of optical coherence tomography compared with intravascular ultrasound and coronary angioscopy. J Am Coll Cardiol 50(10):933–939
26. Finn AV et al (2007) Pathological correlates of late drug-eluting stent thrombosis: strut coverage as a marker of endothelialization. Circulation 115(18):2435–2441
27. Cook S et al (2007) Incomplete stent apposition and very late stent thrombosis after drug-eluting stent implantation. Circulation 115(18):2426–2434
28. Caldera AE et al (2009) Endovascular therapy for left main compression syndrome. Case report and literature review. Chest 135(6):1648–1650
29. Ishigami K et al (2009) Long-term follow-up of neointimal coverage of sirolimus-eluting stents–evaluation with optical coherence tomography. Circ J 73(12):2300–2307
30. Miyoshi N et al (2010) Comparison by optical coherence tomography of paclitaxel-eluting stents with sirolimus-eluting stents implanted in one coronary artery in one procedure.—6-month follow-up. Circ J 74(5):903–908
31. Kim JS et al (2009) Evaluation in 3 months duration of neointimal coverage after zotarolimus-eluting stent implantation by optical coherence tomography: the ENDEAVOR OCT trial. JACC Cardiovasc Interv 2(12): 1240–1247
32. Tamburino C et al (2009) First-in-man 1-year clinical outcomes of the Catania coronary stent system with nanothin polyzene-F in de novo native coronary artery lesions: the ATLANTA (Assessment of the Latest non-thrombogenic angioplasty stent) trial. JACC Cardiovasc Interv 2(3):197–204
33. Bezerra HG et al. (2009) Determining the optimal cross-sectional analysis interval for OCT assessment of coronary stenting. Circulation 120:S1000(Supplement)

34. Terashima M et al (2009) Accuracy and reproducibility of stent-strut thickness determined by optical coherence tomography. J Invasive Cardiol 21(11):602–605
35. Kyono H et al (2010) Optical coherence tomography (OCT) strut-level analysis of drug-eluting stents (DES) in human coronary bifurcations. EuroIntervention 6(1):69–77
36. Okamura T, Serruys PW, Regar E (2010) Three-dimensional visualization of intracoronary thrombus during stent implantation using the second generation, Fourier domain optical coherence tomography. Eur Heart J 31(5):625